

International Journal of Sustainable Energy Planning and Management

System integration of geothermal heat plant in high-temperature district heating system - technical and economic issues

Mariusz Tańczuk^a, Stanisław Anweiler^{a,*}, Sławomir Pochwała^a, Eligiusz Olszewski^b,
Paweł Łuczak^c, Jacek Kalina^d, Stanislav Boldyryev^e

^aDepartment of Mechanical Engineering, Opole University of Technology, Mikołajczyka Str. 5, 45-271 Opole, Poland

^bECO SA, Harcerska Str. 15, 45-118 Opole, Poland

^cECO Kutno Sp. z o.o., Metalowa Str. 10, Kutno,

^dDepartment of Energy and Environmental Engineering, Silesian University of Technology, Konarskiego Str. 18, 44-100 Gliwice, Poland

^eFaculty of Mechanical Engineering and Naval Architecture, University of Zagreb, Zagreb, Croatia

ABSTRACT

Second-generation district heating (DH) systems based on coal combustion remain prevalent and inefficient in Central and Eastern Europe, particularly in Poland. This study investigates the technical and economic feasibility of integrating geothermal energy into an existing high-temperature DH system with a peak demand of 60 MW. Three retrofit scenarios are analyzed: (1) a geothermal doublet with a direct heat exchanger; (2) Scenario 1 extended by an absorption heat pump (AHP) powered by a gas boiler; and (3) Scenario 2 enhanced with an additional geothermal doublet. A detailed hour-by-hour simulation of thermal performance was conducted for each configuration. The share of geothermal heat in total production increases from 35% in Scenario 1 to nearly 70% in Scenario 3, enabling all variants to meet the efficiency thresholds defined in the EU Energy Efficiency Directive. An economic assessment using Net Present Value (NPV) and Internal Rate of Return (IRR) indicates that Scenario 1 is the most cost-effective, yielding an IRR above 17% and a 4-year discounted payback period. Although Scenario 3 achieves higher decarbonization, it requires significantly greater capital investment. The findings highlight that geothermal retrofitting, particularly with direct heat exchangers, offers a realistic and economically justified path for transforming legacy DH systems toward carbon neutrality.

Keywords

District heating;
Geothermal energy;
Retrofit scenarios;
Decarbonization;
Energy efficiency

<http://doi.org/10.54337/ijsepm.9956>

1. Introduction

Modern cities face mounting challenges such as rapid urban growth, environmental stress, social disparities, and rising expectations for public services. In this context, district heating (DH) systems emerge as a cornerstone of sustainable urban energy, driven by climate goals and development principles [1]. Though not a new concept, these systems rapidly evolve to support the transition away from fossil fuels, offering a scalable path to low-carbon, efficient heating infrastructure [2]. The worldwide digital heat market is estimated to be worth

200 billion USD and is projected to expand at an annual growth rate of 5% over the next three years. The growth of the district heating market is driven by an increasing demand for energy efficiency and is supported by strict environmental regulations that promote cleaner heating solutions.

Additionally, the demand is boosted by rising urbanization, which underscores the need for centralized heating solutions [3]. The latest generation of district heating technologies facilitates using low-temperature renewable heat sources [4]. Recent research has focused

*Corresponding author – e-mail: s.anweiler@po.edu.pl

List of Abbreviations		
DH:	District Heating	$\dot{Q}_{DHE,well}$: Heat output of one geothermal well exchanger [MW]
CHP:	Combined Heat and Power	$Q_{GP,i}$: Annual heat output of the geothermal plant in scenario i [MWh]
AHP:	Absorption Heat Pump	$\dot{E}_{CHP,i}$: Instantaneous electrical output of CHP units [MW]
DHE:	Direct Heat Exchanger	$E_{el,GP}^g$: Annual electricity generation of geothermal plant [MWh]
TES:	Thermal Energy Storage	$E_{el,GP}^c$: Annual electricity consumption of geothermal plant [MWh]
EED:	Energy Efficiency Directive (EU)	F_{GP} : Annual fuel consumption of geothermal plant [MWh _{fuel}]
EU ETS:	European Union Emissions Trading System	η_{th} : Thermal efficiency of coal boilers [–]
SET_HEAT:	Supporting Energy Transition and Decarbonisation in District Heating Sector Project	$\eta_{el,CHP}$: Electrical efficiency of CHP units [–]
O&M:	Operation and Maintenance	η_{GB} : Efficiency of gas boiler driving AHP [–]
MPa:	Megapascal	COP_{AHP} : Coefficient of performance of the absorption heat pump [–]
CAPEX:	Capital Expenditure	τ : Time variable [h]
NPV:	Net Present Value	d : Discount rate used in NPV calculation [–]
IRR:	Internal Rate of Return	N : Project lifetime [years]
$\dot{Q}_{coal,i}$	Instantaneous heat output from coal boilers at time step i [MW]	CAPEX: Capital expenditure [€]
$\dot{Q}_{CHP,i}$	Instantaneous heat output from CHP units at time step i [MW]	CF_{τ} : Cash flow in year τ [€]
$\dot{Q}_{DHE,i}$	Instantaneous heat output from direct geothermal heat exchanger at time step i [MW]	NPV: Net Present Value [€]
$\dot{Q}_{AHP,i}$	Instantaneous heat output from absorption heat pump at time step i [MW]	IRR: Internal Rate of Return [%]
		LHV: Lower Heating Value of fuel [MJ/kg]

mainly on optimizing demand management during peak periods, such as peak shaving [5], developing low-emission solutions with the use of multi-energy resources [6], and improving load forecasting methods [7]. Nevertheless, there may be confusion about the simultaneous development of the latest generation of district heating systems, which operate at much lower temperatures than traditional systems [8], [9]. It becomes crucial to define the various fifth-generation district heating and cooling (5GDHC) systems and briefly this cutting-edge technology as discussed in their paper [10].

Discussing the dominance of low-efficiency fossil-fuel-based second-generation district heating systems in some European countries [11], including Poland [12], requires an analysis of the current situation and trends [13]. In many European countries, there is a dominance of low-efficiency second-generation district heating systems, mainly based on fossil fuel use. Several factors, such as the availability of raw materials, existing infrastructure, and energy policy, are involved [14]. Second-generation district heating systems primarily use fossil fuels, especially coal, as the main thermal energy source. In the case of Poland,

most of these systems are based on burning coal, which is a significant part of the country's energy mix [15] (Fig. 1).

The undeniable problem of low-efficiency second-generation district heating systems is their low thermodynamic efficiency. Burning fossil fuels often leads to energy losses, making these systems inefficient and generating large CO₂ emissions. In addition, low-efficiency second-generation district heating systems often fail to meet regulatory requirements for energy efficiency, particularly the Energy Efficiency Directive (EU) 2023/1791 (EED) [17]. This poses a challenge for both local authorities and the energy sector. The existing infrastructure and investments made in the past encourage the continued operation of existing systems. The illustrative locations of efficient and inefficient district heating systems in Poland, in the understanding of the Efficiency Directive, are shown in Figure 2. The graphical illustration of the efficiency requirements as defined in the Energy Efficiency Directive: status quo and the timeline of expected changes are shown in Figure 3.

The drive to optimize the operation of district heating networks is proceeding in multiple directions. For

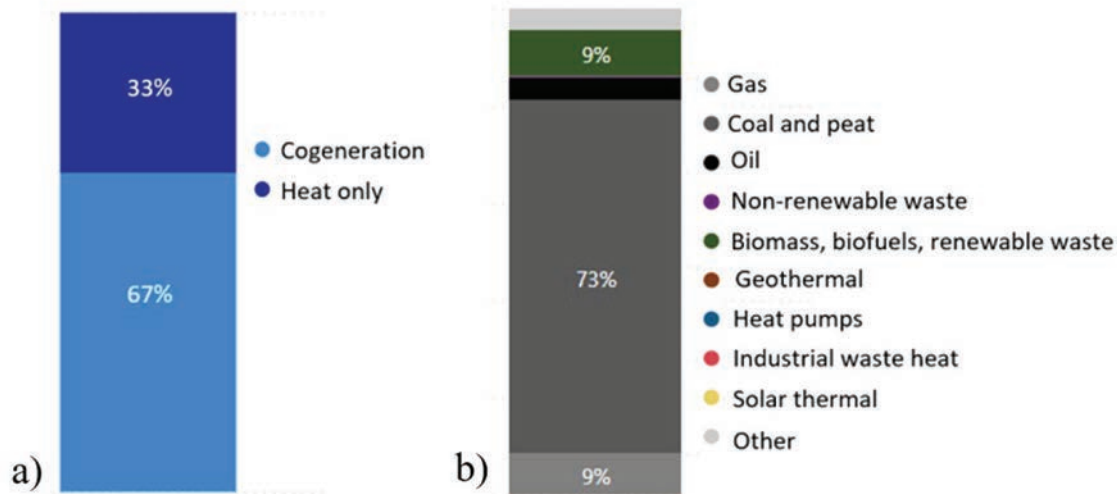


Figure 1: Statistics of the DH sector in Poland: a) district heating supply structure, b) district heating fuel supply mix. Based on data from [16].

example, based on the optimization of building clusters [19], the flexibility of energy storage in district heating pipelines [20], or optimal planning using the thermal inertia of the system [21]. In the paper [22] the authors explore a new business model for the coordinated operation of a wind power plant (WPP) and a flexible district heating system. To find optimal coordination of electricity and heat [23] researchers are pointing out that in the case of geothermal district heating systems, they traditionally dissipate heat and consume excess electricity, prompting the integration of thermal energy storage (TES) to optimize efficiency [24], [25]. The study evaluated 37 parametric cases of an integrated TES

geothermal district heating system using thermodynamic analysis, the net present value (NPV) method for economics, and efficiency analysis with output satisfaction (EATWOS) to determine the most efficient design. In Turkey, for example, such possibilities have been studied and it has been found that district heating systems using geothermal resources will reduce greenhouse gas emissions by 1.58% per year, with an amortization period of about 13 years for a system equivalent to 1,000,000 dwellings [26]. Recent developments in the building sector, district heating and cooling (DHC), and geothermal technology aim to create sustainable and climate-friendly heating and cooling supply systems [27].

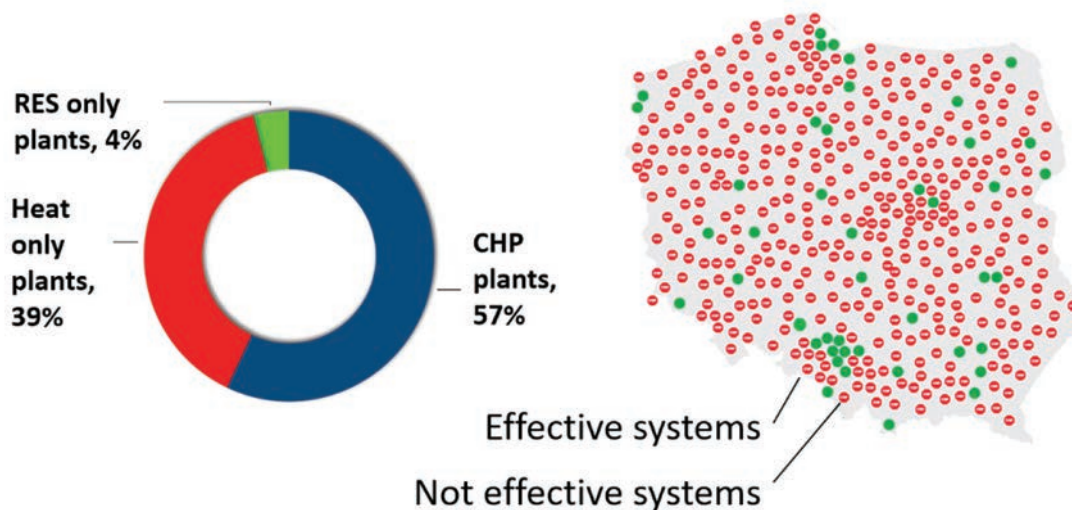


Figure 2: Locations of efficient and inefficient district heating systems in Poland [Reference data [18]].

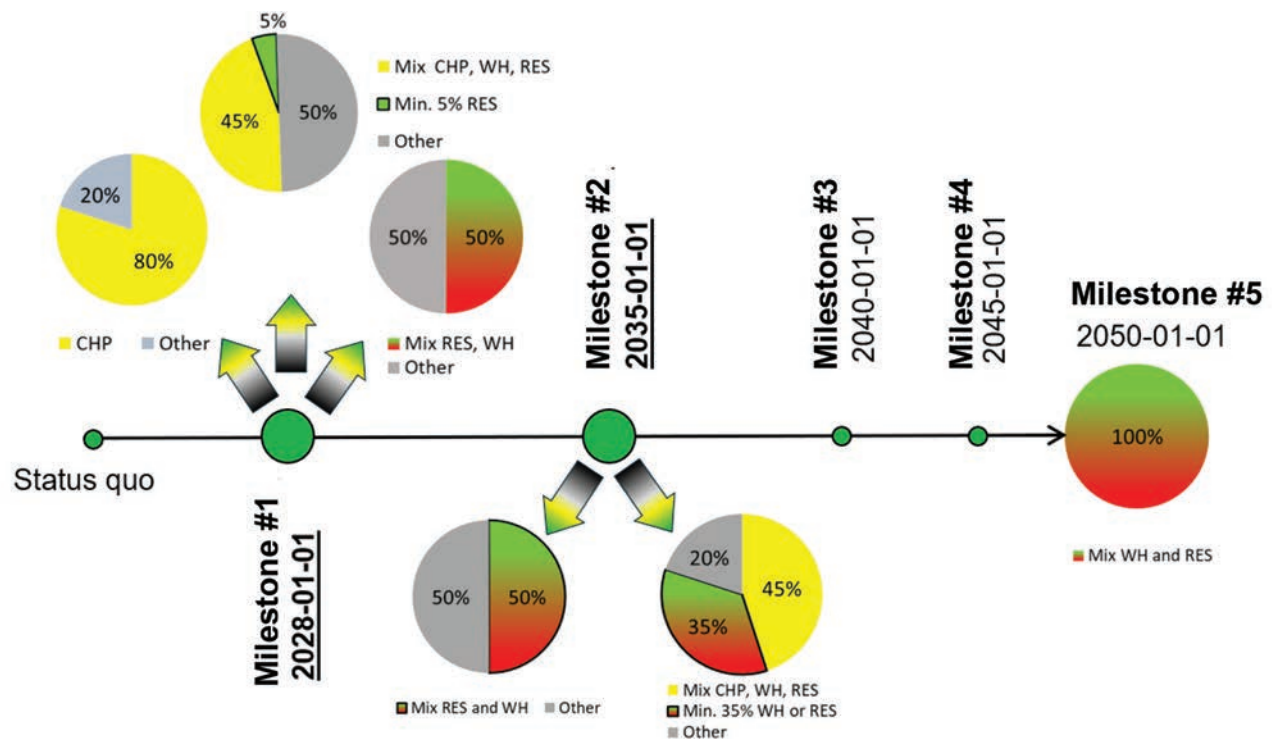


Figure 3: Efficiency criteria of DH systems according to the Energy Efficiency Directive (EED), where, according to the status quo (valid by the year 2028), an efficient system has the following fuel mix: 50% renewable heat, 50% unspecified or 50% waste heat, 50% unspecified or 75% co-generation, 25% unspecified, or 50% mix (CHP, renewables, waste heat) and 50% unspecified.

The work [28], in turn, evaluates the integration of geothermal energy into Geneva's district heating system to decarbonize the heating sector, with a potential contribution of 22% by 2035. In the paper [29] the authors present a drive to modernize the district heating system by integrating modular heat pumps, geothermal water, and PVs to increase flexibility and decentralize the system in Poland. Geothermal energy extraction technologies include Downhole Heat Exchangers (DHE) and Borehole Heat Exchangers (BHE) [30].

Contemporary approaches to planning the transformation of heating systems increasingly use high-resolution heat demand mapping tools, known as heat maps, which enable the assessment of energy efficiency potential in geographical terms, with resolution at the level of individual buildings and distribution networks [31], [32]. At the same time, in Central and Eastern Europe, including Poland, there is a growing need to synchronize local transformation plans with European climate policy objectives, especially in the context of desynchronization from fossil fuel-based transmission systems and integration with the continental system, which requires the

development of system flexibility and operational security [33]. In this context, energy transition models at the municipal and regional levels are becoming increasingly important. These models consider the characteristics of local resources, infrastructure, political and social scenarios, allowing for the design of transition paths to low-carbon systems in an integrated and realistic manner [11].

The current study considers the integration of a renewable heat plant based on geothermal energy into a high-temperature district heating system to partially or fully decarbonize a municipal district heating system with a peak demand of 60 MW. The paper presents the current configuration of the second-generation system and later analyses several potential reconfiguration scenarios based on geothermal resource availability and power system modelling. The technical and economic optimization results indicate that a transition to geothermal energy could be a viable path to a fully decarbonized district heating system.

Previous studies have focused mainly on low-temperature (3rd and 4th generation) systems and the transition to lower temperatures. At the same time, there is a

lack of analysis of the integration of geothermal sources with existing high-temperature systems, particularly in the Polish context. Our study fills this gap by presenting a case study of a water-powered system at temperatures above 100°C. There is also a lack of detailed analyses from Central and Eastern Europe in the literature, despite this region's geological and structural specificity – our analysis provides valuable empirical data from Poland. In addition, although absorption pumps are well known, few studies examine their role in gas heating systems in the context of decarbonization. We have considered this aspect by analysing variants with and without their use. Another novelty is the inclusion of variable energy prices and subsidies in the economic assessment, which allows for a more realistic assessment of the profitability of the investment.

2. System description

The analyzed heat generation plant is a heat source for a high-temperature district heating system with a maximum (peak) heat demand of about 48 MW. Hot water with a nominal pressure of 1.6 MPa and a nominal (maximum) feed temperature of 130 °C is the heat carrier in the district heating network. As presented in Figure 4, the plant remains in operation during the whole year, supplying the city network with heat to provide central heating of residential buildings (in the heating

season) and domestic hot water (in the season and off-season periods). The demand during the off-season is relatively constant: baseload equals ca. 5 MW. The ratio between peak and baseload demand is around 10, which is significant and typical for municipal DH systems operated throughout the year. The data presented in Figures 4, 6, and 7 were obtained from the Supervisory Control and Data Acquisition (SCADA) system of the district heating plant considered in this study.

The district heating system under consideration is supplied by the heat generation plant and divided into two technological parts: a conventional coal-fired source and a gas-fired, highly efficient cogeneration system. The coal facility is based on seven water-stoker boilers, while the cogeneration is one of three IC-engines cogeneration units. A schematic diagram of the system under consideration is shown in Figure 5. The main technical parameters of the existing production units have been presented in Table 1.

Stoker boilers (CSB1 to CSB7) operated in the existing plant in the current configuration are fed up with fine coal of a lower heating value (LHV) between 21 and 22.5 MJ/kg. Three cogeneration units based on IC engines are supplied with nature and connected to the DH network's return pipeline. The historical heat output of the operated units is the base for further simulations. The hour-by-hour load of the existing coal boilers and gas CHP units is presented in Figure 6 and

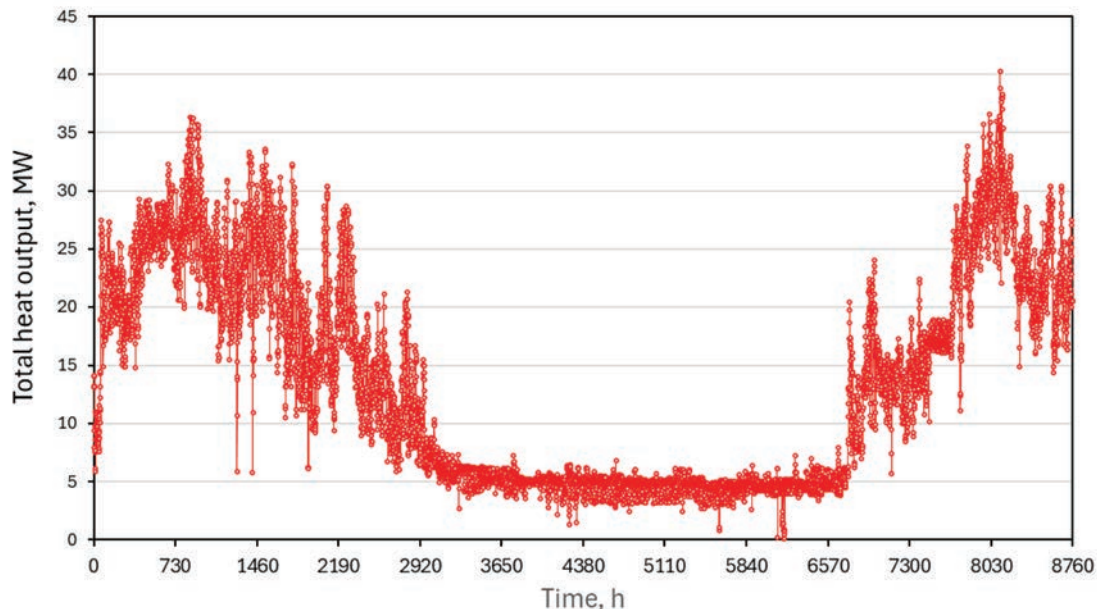


Figure 4: Heat demand of analysed DH system - a real-time hour-by-hour data of heat demand, based on data from SCADA system of the plant under consideration.

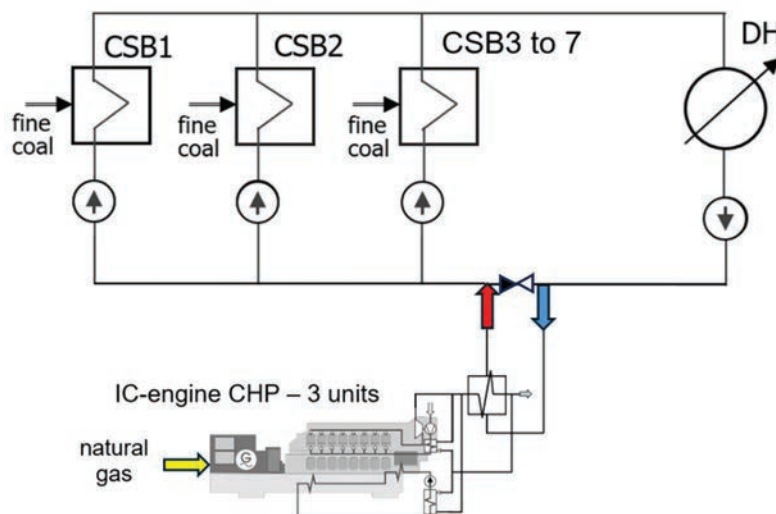


Figure 5: Simplified schematic diagram of DH plant – status quo configuration.

Table 1: Main technical parameters of existing stoker boilers.

Unit	Type	Rated output power, MW	Nominal thermal power in fuel, MW	Overloading capacity, MW	Design efficiency, %
CSB1	WR-5/EM - stoker boilers, equipped with economizer	6.00	6.78	7.50	88.5
CSB2		6.00	6.94	8.00	88.5
CSB3		6.00	6.78	8.00	88.5
CSB4		6.00	6.94	8.00	88.5
CSB5		6.00	6.78	7.50	88.5
CSB6		6.00	6.78	7.50	88.5
CSB7	WR-5 - stoker boiler	5.82	7.09	7.00	82.1
Coal boilers – total		41.82	48.09	53.2	-
CHP1	IC-based CHP unit fired with natural gas	2.2/2.0	4.86	-	86.4
CHP1		2.2/2.0	4.86	-	86.4
CHP3		2.2/2.0	4.86	-	86.4
Gas CHP units - total		3.60	14.58	-	-

the heat load duration curve is presented in Figure 7. As can be seen, the base load of system heat demand is covered by the CHP plant which is the only unit working in the summer period, when the heat demand reaches almost 5 MW. In the period when heating demand begins to grow, the coal boilers start operating. According to historical data, the CHP plant operates nearly year-round, supplying heat to the municipal grid. CHP units operate from about 8 200 to 8 400 hours per year. From the data presented in Figure 6 and Figure 7, it can also be observed that there are periods of reduced operation of the gas CHP during high heat

demand. Temporary or short-term reductions of the gas CHP loads recorded in the operational data acquisition system result from planned system downtime or the necessary decrease of CHP capacity due to the technical minimum requirements of the coal-fired boilers being operated simultaneously with the CHP unit.

Reconfiguration concepts of the ineffective DH system have to face different challenges specific to using geothermal energy for district heating systems. In general, the following critical issues can be specified regarding DH application, specific to the circumstances in the given location (Poland):

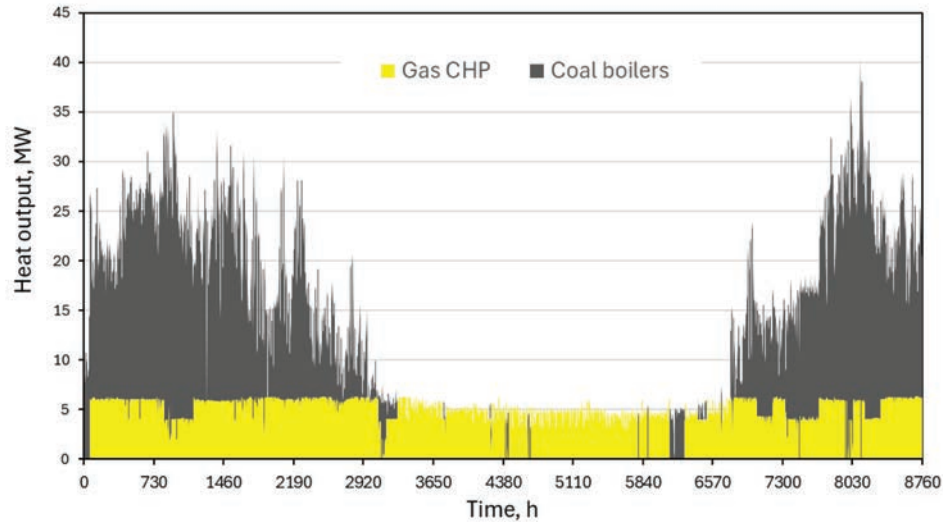


Figure 6: A real-time hour-by-hour heat output of the existing units, based on data from SCADA system of the plant under consideration.

- relatively low temperature of available geothermal water resources, generally 40–70°C, maximum 80-90 °C;
- the need to perform deep boreholes, sometimes several kilometres;
- limited flow and thermal efficiency of the resource (geothermal water).

Regarding geological structure, the analysed DH plant is located in the Polish Lowlands, in the axial part of the Kuyavian section of the midland dike (Figure 8). The Polish Lowlands is the largest geothermal region in Poland by area. Geothermal resources here are primarily

associated with Mesozoic Lower Cretaceous and Lower Jurassic reservoirs. Aquifers are formed by sandstone formations with good reservoir parameters, which, combined with the deep location of these formations and their considerable thickness, make it possible to obtain high yields of thermal waters with sufficiently high temperatures for use in heating.

For configurations of wells used in recovering geothermal heat for district heating purposes, it should be noted that a geothermal doublet design is essential. Re-injecting geothermal water is mandatory to prevent reservoir pressure drops, water wastage, and pollution of surface waters

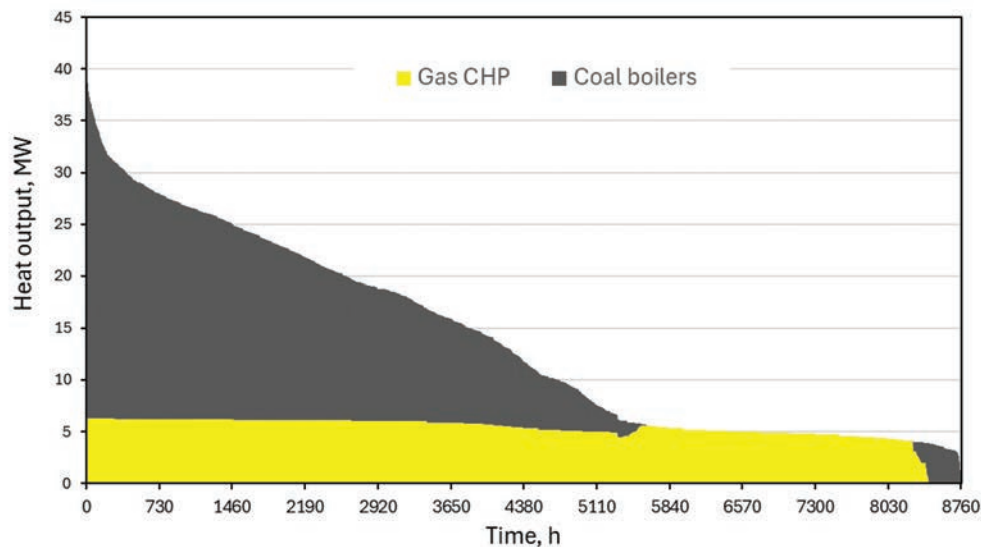


Figure 7: A load duration curve of the operation of the existing units, based on data from SCADA system of the plant under consideration.

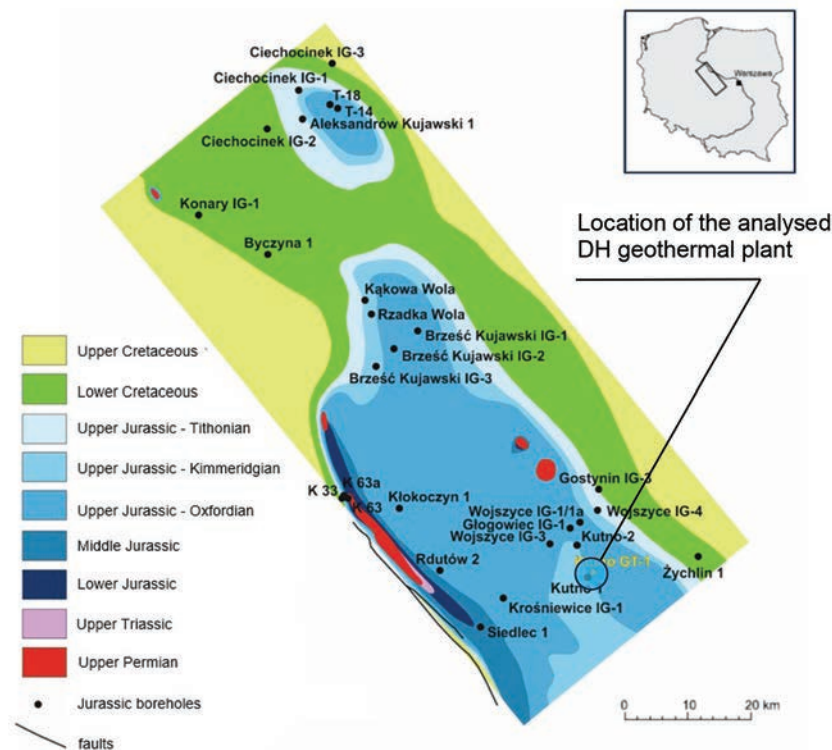


Figure 8: Approximate location of the considered geothermal plant on the background of the geological structure of the Kuyavian dike with the distribution of deep boreholes [34].

if the fluid is rich in minerals. Assuming sufficient reservoir depth, the standard design involves drilling two wells - typically deviating from the same platform to minimize surface land use and reduce the need for surface-level geothermal water transportation. The simplified technological layout of the geothermal plant integrated into the structure of the existing DH plant is presented in Figure 9. There is a direct heat exchanger and an absorption heat pump recovering heat from the geothermal water taken from the production well.

For the research, it was also assumed that in the area of the current DH plant, it is possible to capture thermal waters with a temperature at the outflow of about 90°C with a borehole (production well) capacity of at least 150 m³/h.

3. Methods and input data

The assumption of the analysis was to retrofit the existing fossil-fuel-based DH system with the deep geothermal plant according to different configuration scenarios. The study's basic premise was based on the assumption that recoverable renewable geothermal heat could be obtained

from deep (about 3 km) wells directly using heat exchangers or an absorption heat pump driven by heat produced in a gas boiler. The capacity of the geothermal well was also a variable quantity in the simulations. The following three reconfiguration scenarios were adopted for further analysis (Figure 10 and Table 2):

- Scenario 1 is based on one geothermal doublet of wells with a direct heat exchanger,
- Scenario 2 is based on one geothermal doublet of wells with a direct heat exchanger and an absorption heat pump unit supplied with hot water from a gas boiler,
- Scenario 3 is based on two geothermal doublets of wells with a direct heat exchanger and an absorption heat pump unit supplied with hot water from a gas boiler.

The decision to include a natural gas-fired absorption heat pump in the Scenario 2 was based on the availability of gas infrastructure on site and the role of natural gas as a transitional fuel recognized in EU climate policy. Natural gas is currently used in high-efficiency cogeneration at the plant and is available in sufficient quantity for

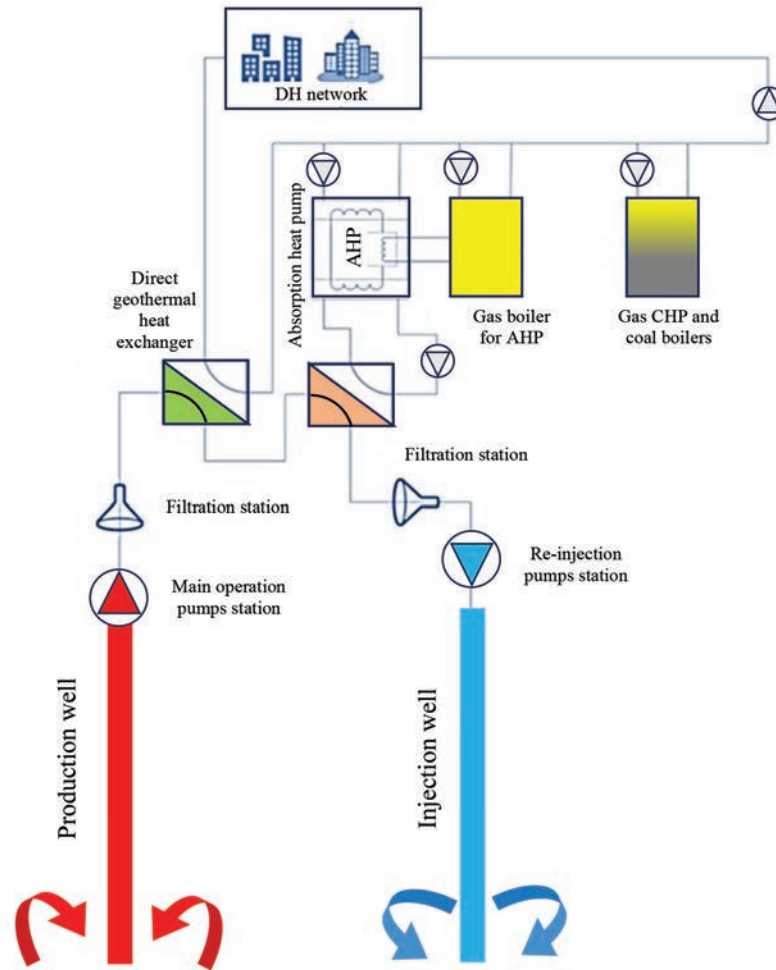


Figure 9: Technical layout of the geothermal plant integrated into a coal and gas-based DH plant.

use in the absorption heat pump. Furthermore, the use of gas-driven absorption heat pumps can be considered environmentally responsible due to their use of natural refrigerants (e.g., ammonia-water systems) with zero Ozone Depletion Potential ($ODP = 0$) and Global Warming Potential ($GWP = 0$). Given the investment's relatively short economic payback time (less than 4–5 years for all scenarios), the gas-driven solution can be considered a practical transitional step towards deeper decarbonization, especially considering that biomethane or green hydrogen may become available within this timeframe.

It should also be noted here that coal boilers remain as peak units in each scenario. In cases with an absorption heat pump, no cogeneration units are left.

Simplified configurations of the plant for analyzed retrofitting scenarios: a) Scenario 1, b) Scenarios 2 and 3 are shown in Figure 10.

As Figure 10 shows in Scenario 1, the geothermal source is connected to the DH grid via a direct heat exchanger without an absorption heat pump. Due to the limited supply temperature of the geothermal water ($90\text{ }^{\circ}\text{C}$), this configuration alone would not be sufficient to meet the highest temperature requirements of the DH network. Therefore, it is assumed that the coal boilers will be activated during peak demand periods or when higher supply temperatures are needed to supplement the heat supply. This ensures continuous system operation and compliance with temperature constraints of the existing DH infrastructure. The coal boilers remain backup and peak units in all scenarios, reflecting a realistic hybrid system configuration typical for transition-phase DH systems.

Based on assumed technical configurations of the plant, the design parameters of applied units, and the

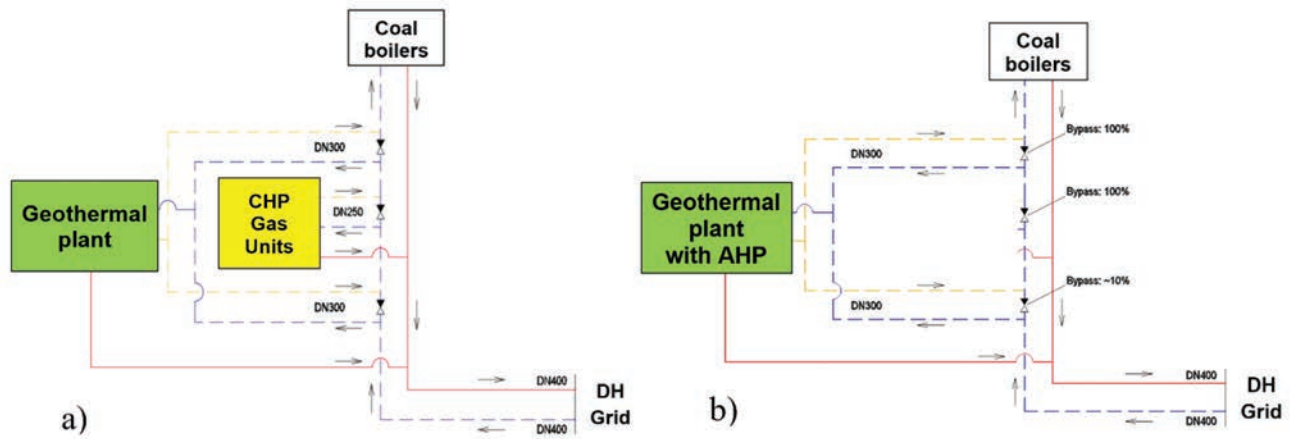


Figure 10: Simplified configuration of the plant for analyzed retrofitting scenarios: a) Scenario 1, b) Scenarios 2 and 3.

Table 2: Main technical parameters of the DH plant after retrofitting with a geothermal facility.

Retrofitting scenario	Fuel	Installed thermal power, MW	Installed electrical power, MW
S1	Coal boilers	41.8	-
	CHP - natural gas	6.0	6.6
	Direct heat exchanger - geothermal energy	6.3	-
Total		54.1	6.6
S2	Coal boilers	41.8	-
	Absorption heat pump driven by gas boiler	13.0	-
	Direct heat exchanger - geothermal energy	6.3	-
Total		61.1	-
S3	Coal boilers	41.8	-
	Absorption heat pump driven by gas boiler	13.0	-
	Direct heat exchanger - geothermal energy	12.6	-
Total		67.4	-

given load duration curve, an hour-by-hour simulation of the plant's annual operation was conducted for each scenario case. The hourly simulation of the district heating plant was performed for all scenarios (8760 h/year), based on real demand data and technical parameters of each unit. Heat and fuel flows were calculated using thermodynamic balances and device efficiencies. As a result, the annual heat production $Q_{GP,i}$ and electricity production $E_{el,GP}^g$ and consumption $E_{el,GP}^c$ of the DH plant was derived with the use of the following formulas:

$$Q_{GP,i} = \int_{\tau=0}^{\tau=8760} (\dot{Q}_{coal,i}) d\tau + \int_{\tau=0}^{\tau=8760} (\dot{Q}_{CHP,i}) d\tau + \int_{\tau=0}^{\tau=8760} (\dot{Q}_{DHE,i}) d\tau + \int_{\tau=0}^{\tau=8760} (\dot{Q}_{AHP,i}) d\tau$$

$$E_{el,GP}^g = \int_{\tau=0}^{\tau=8760} (\dot{N}_{CHP,i}) d\tau$$

$$E_{el,GP}^c = \int_{\tau=0}^{\tau=8760} (\dot{N}_{GP,i}) d\tau$$

The fuel consumption of the analysed plant was derived from:

$$F_{GP} = \int_{\tau=0}^{\tau=8760} (\dot{F}_{coal,i}) d\tau + \int_{\tau=0}^{\tau=8760} (\dot{F}_{CHP,i}) d\tau + \int_{\tau=0}^{\tau=8760} (\dot{F}_{AHP,i}) d\tau$$

where the fuel consumption of the analyzed coal units $\dot{F}_{coal,i}$, natural gas cogeneration units $\dot{F}_{CHP,i}$ and the absorption heat pump unit $\dot{F}_{AHP,i}$ was calculated based on the following formulas:

$$\dot{F}_{coal,i} = (\dot{Q}_{coal,i} / \eta_{th})$$

$$\dot{F}_{CHP,i} = (\dot{N}_{CHP,i} / \eta_{el,CHP})$$

$$\dot{F}_{AHP,i} = (\dot{Q}_{AHP,i} / (COP_{AHP,i} * LHV * \eta_{GB,i}))$$

The proximate values of heat and electricity flow for a particular hour of the DH plant operation have been provided by the simulation procedure conducted for the i -th case of the reconfiguration scenario. In the case of heat generated from geothermal resources through the direct heat exchanger, the heat output $\dot{Q}_{DHE,well}$ in a particular hour, it was determined on the assumption that the production from one well of the capacity of 150 m³/h and the geothermal water temperature of 90 °C. It was estimated using a sixth-degree polynomial Eq. (8) and chart in Figure 11), which was obtained by fitting a trend line to the results of hourly simulation data derived from the assumed operating profile of the system. The input dataset consisted of heat transfer values calculated based on assumed geothermal water parameters (flow rate and

temperature) and operational constraints. The polynomial function reflects the empirical relationship between the system's hourly operation (represented by time step τ) and the achievable heat output under stable flow and temperature conditions. This approach allows for a simplified yet accurate approximation of geothermal heat contribution in the annual simulation.

$$\dot{Q}_{DHE,well} = -7 \cdot 10^{-22} \cdot \tau^6 + 2 \cdot 10^{-22} \cdot \tau^5 - 2 \cdot 10^{-13} \cdot \tau^4 + 10^{-9} \cdot \tau^3 - 3 \cdot 10^{-6} \cdot \tau^2 + 0.0035 \cdot \tau + 3.5672$$

Following the presented method, the thermodynamic evaluation was the basis for further economic analysis. The goal of the calculation procedure was to find the best configuration of the DH plant (optimal geothermal plant configuration within the analyzed cases) regarding the economic feasibility. The performed economic evaluation based on the discounted method, with Net Present Value (NPV) as the result of the calculations:

$$NPV(\tau = N) = -CAPEX + \sum_{\tau=1}^N \frac{CF_{\tau}}{(1+d)^{\tau}}$$

where a lifetime of the project N was assumed as 15 years, and the annual cash flow CF for a particular year τ was calculated based on Eq. (10).

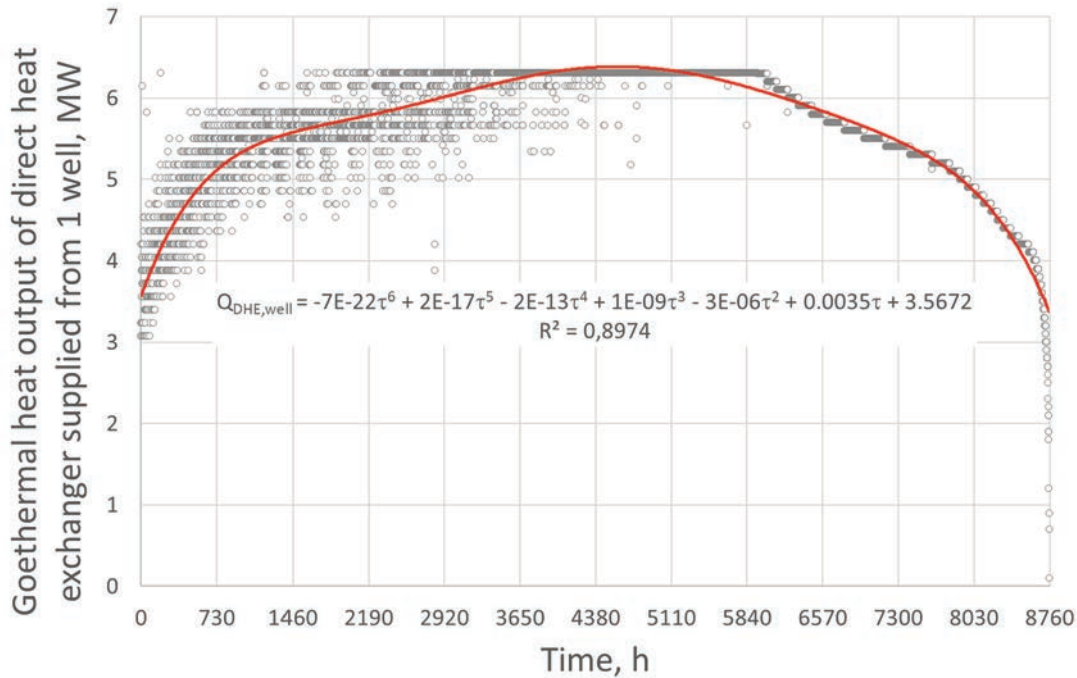


Figure 11: The annual operation curve of the capacity of a direct geothermal heat exchanger under analysis.

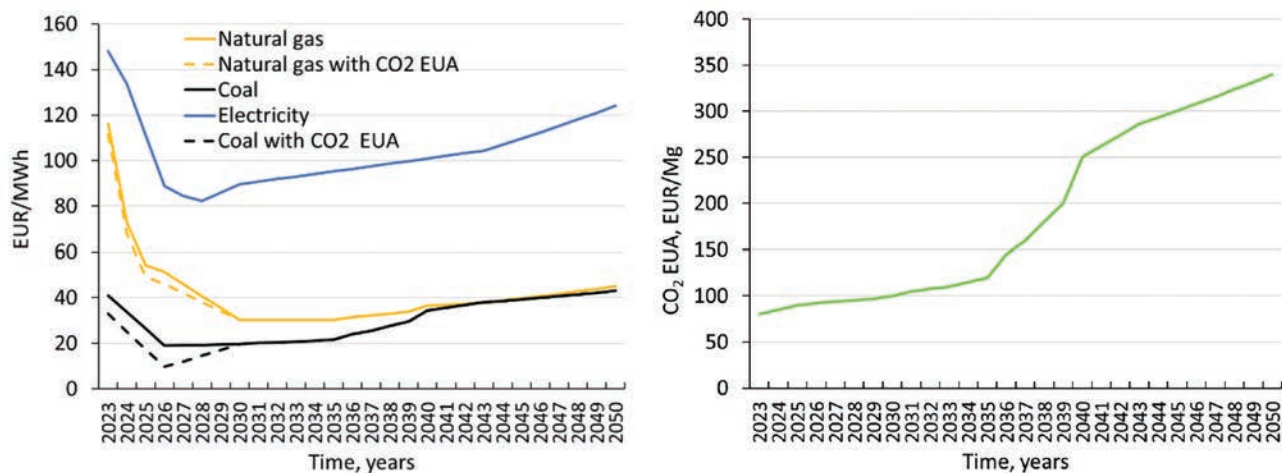


Figure 12: Fuel, electricity, and CO₂ EUA path prices – forecast by 2050.

$$CF_{\tau} = C_{\tau} + S_{\tau}$$

C_{τ} are the annual costs of operation, including electricity costs (mainly pumping), natural gas costs (for the CHP and gas boiler supplying AHP), and maintenance costs (O&M), S_{τ} is the annual sale income generated by electricity sales (only in case of Scenario 1) as well as cutting down operational costs of coal-fired boilers (coal price and O&M costs) and the annual incomes from avoiding costs of buying CO₂ EUA allowances.

The assumed 15-year analysis period reflects an economic assessment horizon rather than the technical lifetime of the geothermal system. While the actual operational lifespan of geothermal infrastructure typically exceeds 25–30 years, 15 years was selected to align with the typical planning and financing cycles for DH retrofit projects in Poland, and to enable a conservative evaluation of investment feasibility.

Apart from the NPV index, the Internal Rate of Return (IRR) index was also derived within the analysis by the iteration formula:

$$NPV|_{d=IRR} = 0$$

To substantiate the results of the economic analysis and take into account changing financial circumstances, it was carried out for variable prices, according to the price and cost paths developed for this purpose. The price path projection up to 2050 was generated and used within the calculations, according to data presented in Figure 12.

The prices presented in Figure 12 are long-term projections. These forecasts incorporate expected trends in energy markets and policy-driven cost developments but

do not include general inflation or short-term (hourly or daily) market volatility. For this study, energy procurement is assumed to be based on long-term supply contracts with fixed pricing structures that follow projected average annual trends. Moreover, hourly fluctuations in electricity or gas prices were not considered, as the focus of the economic assessment is on the strategic planning level and not on operational market optimization.

In the case of geothermal projects, receiving a subsidy is very likely, hence the assumption of a subsidy of between 50% and 55% of expected CAPEX was used for the calculations. A discount rate $d = 7.5\%$ was assumed for discount calculations.

This assumption on subsidy is based on the availability of dedicated national and EU co-financing programs that support the integration of renewable energy sources into district heating systems in Poland. In particular, geothermal energy projects are eligible for grants under schemes such as the National Fund for Environmental Protection and Water Management (NFOŚiGW) and EU-funded initiatives under the LIFE Programme, Cohesion Fund, and Just Transition Fund. These programs typically offer support covering 50–60% of eligible CAPEX, especially for projects that contribute to decarbonization of municipal infrastructure. Therefore, the assumed subsidy range reflects realistic and documented funding levels for such investments in the Polish context.

4. Results and discussion

Based on the presented method and given input data the thermodynamic simulations were made for three cases

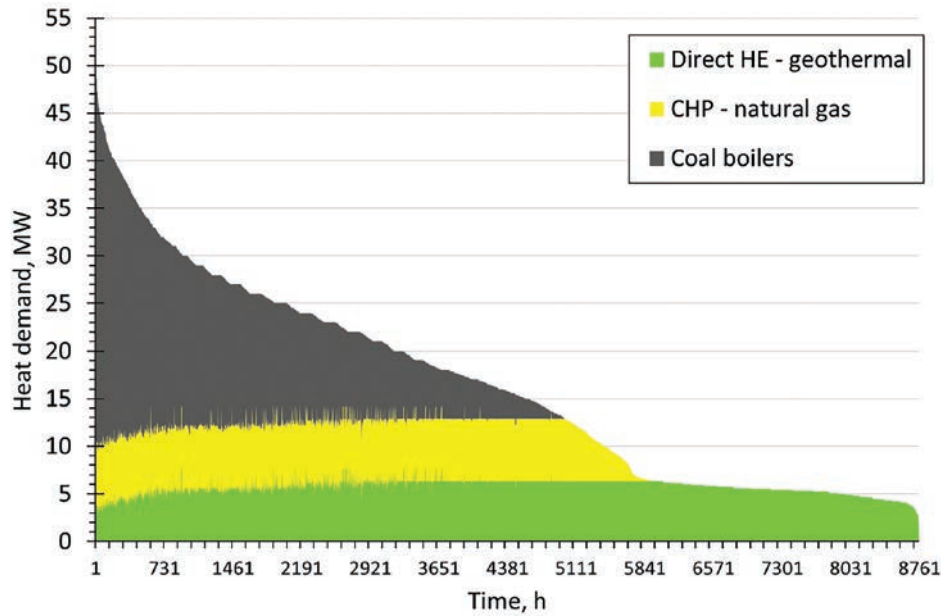


Figure 13: Results of the simulation of the annual operation of the DH plant conducted for the retrofitting Scenario 1.

of different geothermal plant configuration scenarios. The results in the form of the heat load duration curves are presented in Figures 13, 14, and 15.

The plant configuration and size of the units result in the amount of electricity and heat production, fuel consumption, and other operational parameters. Based on conducted simulations, the resulting fuel mix in the total amount of heat delivered to the system for each of

the analyzed scenarios was obtained. As can be seen in Figure 16, the share of heat generated from geothermal resources is increasing along with subsequent scenarios. In the first Scenario, it is equal to 34.8%, while in Scenario 2 and 3, where an absorption heat pump is applied, it goes up to 77.6% and 88.7% respectively.

In the case of Scenario 1, although the geothermal source alone does not cover the full supply temperature

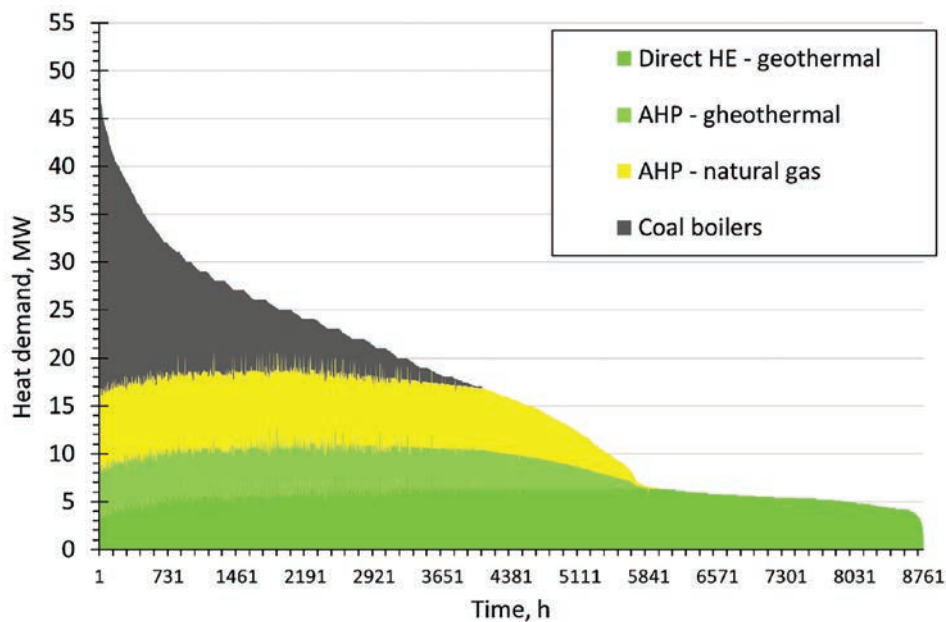


Figure 14: Results of the simulation of the annual operation of the DH plant conducted for the retrofitting Scenario 2.

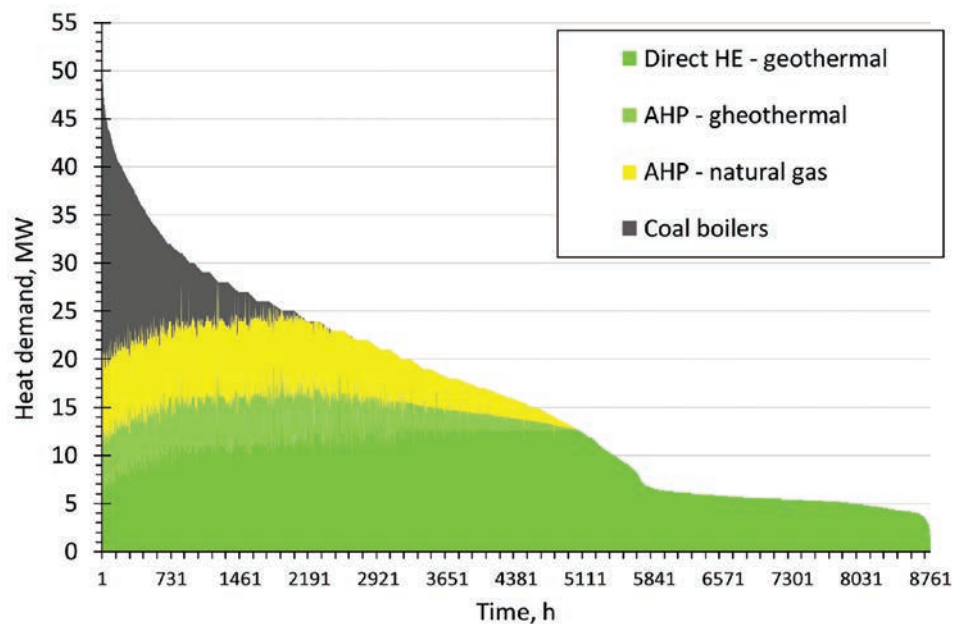


Figure 15: Results of the simulation of the annual operation of the DH plant conducted for the retrofitting Scenario 3.

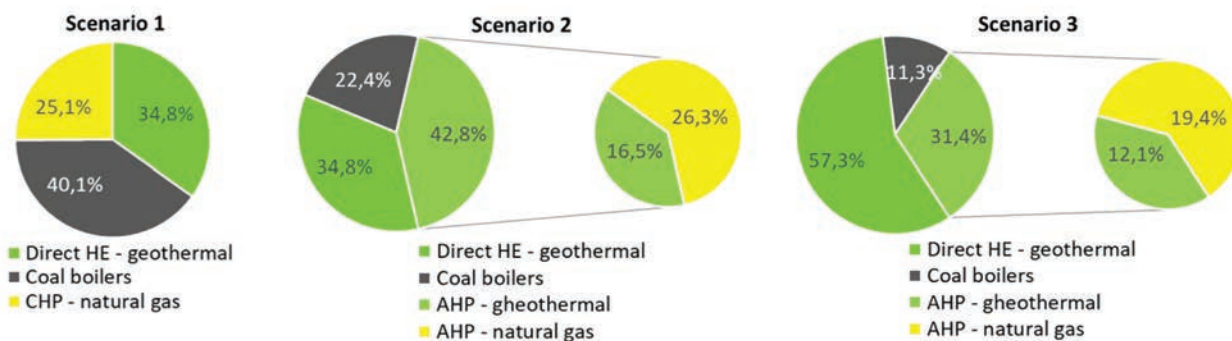


Figure 16: Annual fuel mix achieved for the assumed reconfiguration scenarios.

range, the use of peak-load coal boilers provides the necessary flexibility. This hybrid configuration ensures that the DH system operates reliably throughout the year despite the temperature limitations of the geothermal water. It is worth noting that even without the absorption heat pump, the integration of geothermal heat via direct exchange contributes significantly to system decarbonization and efficiency improvement.

It is also worth noting that in the case of using a heat pump, the amount of renewable heat extracted in the geothermal system under study is less than the heat produced by the heat pump, due to the need to use a non-renewable

medium to drive the pump. In the case analyzed, this is natural gas. With this in mind, the amount of renewable heat generated in each scenario will amount to: 34.8% (Scenario 1), 51.3% (Scenario 2), and 69.4% (Scenario 3). In all analyzed scenarios, the DH system under investigation will gain the status of an effective system meeting the efficiency criteria according to the EED directive.

The summary of main operational data, used as input data to further economic analysis can be found in Table 3.

Based on the data generated from the simulation of the operation of individual cases of DH systems and financial input to the analysis, a cost-effectiveness analysis was

Table 3: Basis annual operational data derived for each reconfiguration case.

Retrofitting scenario	Fuel	Heat production, MWh	Electricity production, MWh	Fuel mix, %
S1	Coal boilers	57 510	0	40,1%
	Natural gas	35 973	32 703	25,1%
	Geothermal energy	49 958	0	34,8%
Total		143 440	6.94	100
S2	Coal boilers	32 093	-	22,4%
	Natural gas	37 779	-	26,3%
	Geothermal energy	73 569	-	51,3%
Total		143 440	-	100
S3	Coal boilers	16 157	-	11,3%
	Natural gas	27 758	-	19,4%
	Geothermal energy	99 526	-	69,4%
Total		143 440	-	100

carried out using the discount method. The NPV of the project for three assumed reconfiguration scenarios is depicted in Figure 17. As can be seen from Figure 17, the shortest payback is for Scenario 1 and 2 where the smallest CAPEX is required. Scenario 3, with additional geothermal doublets of wells, despite the most significant increase in green heat production, it is the least profitable, although still very beneficial (discounted payback time around 4 years). However, it should be noted that NPV

values after 15 years of operation, are almost equal for Scenario 3 and Scenario 2 (around 21 million €).

A summary of the conducted analysis is presented in Table 4. The economic indicators prove that the feasibility of each analyzed scenario is acceptable. Net Present Values after 15 years of operation and the Internal Rate of Return (IRR) values are high. The optimal scenario regarding these parameters is the first case of the proposed reconfiguration: one pair of wells and a direct

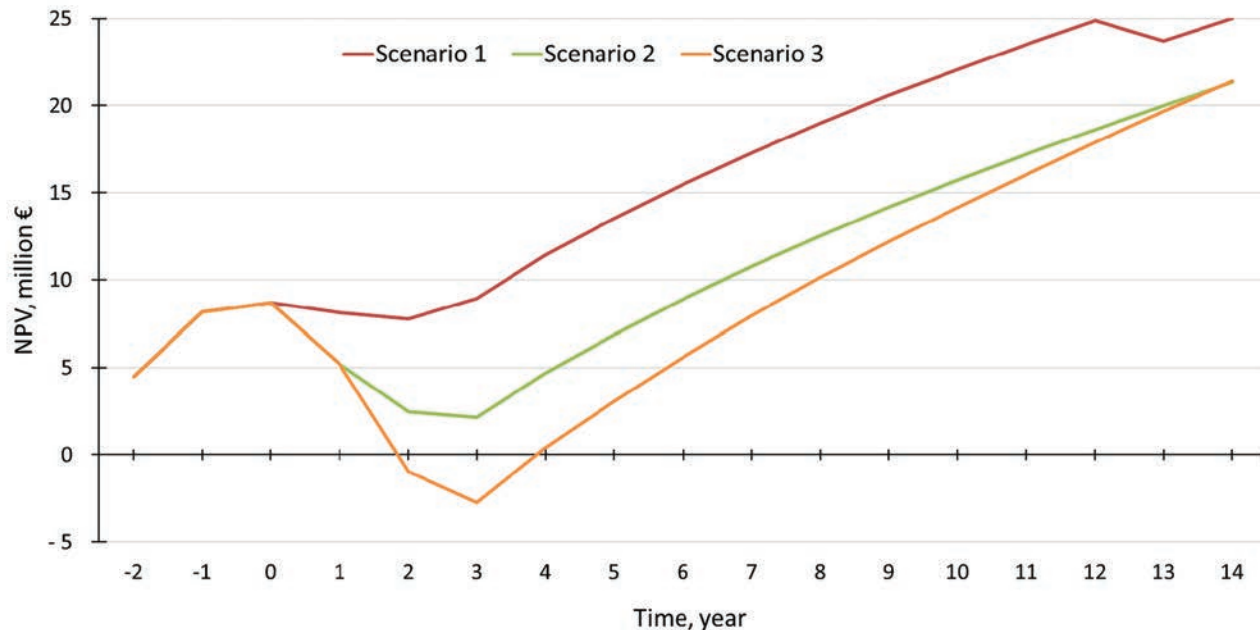


Figure 17: Net Present Value curves for analyzed geothermal plant scenarios.

Table 4: Chosen results of the calculations of feasibility.

Retrofitting scenario	CAPEX, million €	Subsidy, million €	NPV(15), million €	IRR, %
S1	23.844	11.922	25.005	17.3%
S2	35.467	20.116	21.305	10.5%
S3	49.800	27.713	21.414	10.6%

geothermal heat exchanger coupled with existing coal boilers and gas-based CHP units. In this case, NPV(15) exceeds 25 million € and the IRR is higher than 17%.

In complement to the discussion regarding the selected time horizon for analysis, it is essential to note that the investment is highly profitable within this timeframe, and extending the time horizon would only increase the Net Present Value without changing the overall investment decision. The choice of 15 years also reflects expected changes in regulatory, market, and technology frameworks, which may justify re-evaluation of the system in the future.

5. Conclusion and recommendations

This paper considers the integration of a renewable heat plant based on geothermal energy into a high-temperature district heating system as a means to partially or fully decarbonize a municipal district heating system, depending on the assumed reconfiguration scenario. The current configuration of the second-generation system is presented, and various potential scenarios for its reconfiguration are proposed based on available geothermal resources and the system's energy modeling. The technical and economic optimization results show that the geothermal transition path can be a beneficial solution of transformation, enabling transition into a fully decarbonized system meeting efficiency criteria.

The analyses indicate that the most favorable variant for implementing an investment is related to the use of the direct heat exchanger system for recovering geothermal resources. Adding an absorption heat pump unit driven by high-parameter water from a gas boiler (Scenario 2) reduces the profitability of the plant retrofitting.

The recommended variant can be developed by drilling and attaching a second double of geothermal boreholes to the system, which will significantly increase the coverage of heat demand of the district heating system by a renewable energy source. However, even if the additional doublet of geothermal wells is considered (Scenario 3), the profitability of such a variant is still lower than in the case of Scenario 1.

Acknowledgment

The presented research was conducted within the frame of the SET_HEAT project, number 101119793, acronym LIFE22-CET-SET_HEAT, co-funded by the European Union.

References

1. P. A. Østergaard and P. C. Maestosi, "Special Issue: Tools, technologies and systems integration for the Smart and Sustainable Cities to come," *International Journal of Sustainable Energy Planning and Management*, vol. 24, 2019, <https://doi.org/10.5278/ijsepm.vol24>.
2. S. Nielsen *et al.*, "Heating Sector Strategies in Climate-Neutral Societies," *International Journal of Sustainable Energy Planning and Management*, vol. 43, pp. 101–122, Jan. 2024, <https://doi.org/10.54337/IJSEPM.8554>.
3. "District Heating Market Size, Share, Trends, Growth and Industry Analysis - 2028." https://www.marketsandmarkets.com/Market-Reports/district-heating-market-107420661.html?gad_source=1&gclid=Cj0KCQjw5cOwBhCiARIsAJ5njua5nI97tSA711cTO6XXuJPqvKhKM6n_T2K66-IZE8vXdfg3SnCs4E4IaI9BEALw_wcB (accessed Apr. 13, 2024).
4. R. Lund, D. S. Østergaard, X. Yang, and B. V. Mathiesen, "Comparison of Low-temperature District Heating Concepts in a Long-Term Energy System Perspective," *International Journal of Sustainable Energy Planning and Management*, vol. 12, pp. 5–18, Mar. 2017, <https://doi.org/10.5278/IJSEPM.2017.12.2>.
5. U. Trabert, F. Pag, J. Orozalieva, U. Jordan, and K. Vajen, "Peak shaving at system level with a large district heating substation using deep learning forecasting models," *Energy*, vol. 301, p. 131690, Aug. 2024, <https://doi.org/10.1016/J.ENERGY.2024.131690>.
6. T. Zhang *et al.*, "Research on performance and potential of distributed heating system for peak shaving with multi-energy resource," *Sci Rep*, vol. 14, no. 1, pp. 1–21, Dec. 2024, <https://doi.org/10.1038/S41598-024-76108-3>; SUBJMETA=166,4073,4099,639,986; KWRD=CIVIL+ENGINEERING, POWER+DISTRIBUTION.

7. P. Hua, H. Wang, Z. Xie, and R. Lahdelma, "District heating load patterns and short-term forecasting for buildings and city level," *Energy*, vol. 289, p. 129866, Feb. 2024, <https://doi.org/10.1016/J.ENERGY.2023.129866>.
8. A. I. Ianakiev, J. M. Cui, S. Garbett, and A. Filer, "Innovative system for delivery of low temperature district heating," *International Journal of Sustainable Energy Planning and Management*, vol. 12, pp. 19–28, Mar. 2017, <https://doi.org/10.5278/IJSEPM.2017.12.3>.
9. M. A. Ancona, M. Bianchi, L. Branchini, A. De Pascale, F. Melino, and A. Peretto, "Low temperature district heating networks for complete energy needs fulfillment," *International Journal of Sustainable Energy Planning and Management*, vol. 24, pp. 33–42, Oct. 2019, <https://doi.org/10.5278/IJSEPM.3340>.
10. L. M. Dang *et al.*, "Fifth generation district heating and cooling: A comprehensive survey," *Energy Reports*, vol. 11, pp. 1723–1741, Jun. 2024, <https://doi.org/10.1016/J.EGYR.2024.01.037>.
11. K. Gupta and E. O. Ahlgren, "Analysis of City Energy Systems Modeling Case Studies: A Systematic Review," *International Journal of Sustainable Energy Planning and Management*, vol. 43, no. 123, pp. 123–139, Jan. 2024, <https://doi.org/10.54337/IJSEPM.9335>.
12. M. Widziński, P. Chaja, A. N. Andersen, M. Jaroszevska, S. Bykuć, and J. Sawicki, "Simulation of an alternative energy system for district heating company in the light of changes in regulations of the emission of harmful substances into the atmosphere.," *International Journal of Sustainable Energy Planning and Management*, vol. 24, pp. 43–56, Oct. 2019, <https://doi.org/10.5278/IJSEPM.3354>.
13. M. A. Sayegh *et al.*, "Trends of European research and development in district heating technologies," *Renewable and Sustainable Energy Reviews*, vol. 68, pp. 1183–1192, Feb. 2017, <https://doi.org/10.1016/J.RSER.2016.02.023>.
14. P. A. Østergaard, R. M. Johannsen, N. Duic, and H. Lund, "Sustainable Development of Energy, Water and Environmental Systems and Smart Energy Systems," *International Journal of Sustainable Energy Planning and Management*, vol. 34, pp. 1–4, May 2022, <https://doi.org/10.54337/IJSEPM.7269>.
15. E. Hałaj, J. Kotyza, M. Hajto, G. Pelka, W. Luboń, and P. Jastrzębski, "Upgrading a District Heating System by Means of the Integration of Modular Heat Pumps, Geothermal Waters, and PVs for Resilient and Sustainable Urban Energy," *Energies* 2021, Vol. 14, Page 2347, vol. 14, no. 9, p. 2347, Apr. 2021, <https://doi.org/10.3390/EN14092347>.
16. "DHC Trend - IREES GmbH." <https://irees.de/2021/10/18/district-heating-and-cooling-trend-interactive-report/> (accessed Jun. 17, 2025).
17. "Official Journal of the European Union. DIRECTIVE (EU) 2023/1791 OF THE EUROPEAN PARLIAMENT AND OF THE COUNCIL of 13 September 2023 on energy efficiency and amending Regulation (EU) 2023/955 (recast)." <https://eur-lex.europa.eu/eli/dir/2023/1791/oj/eng> (accessed Jun. 17, 2025).
18. M. Ziarkowski, "Opportunities and directions in the transformation of district heating in Poland," *internetowy Kwartalnik Antymonopolowy i Regulacyjny (internet Quarterly on Antitrust and Regulation)*, vol. 9, no. 6, pp. 28–42, Jul. 2020, <https://doi.org/10.7172/2299-5749.IKAR.6.9.2>.
19. L. Pompei, J. Mannhardt, F. Nardecchia, L. M. Pastore, and L. de Santoli, "A Different Approach to Develop a District Heating Grid Based on the Optimization of Building Clusters," *Processes* 2022, Vol. 10, Page 1575, vol. 10, no. 8, p. 1575, Aug. 2022, <https://doi.org/10.3390/PR10081575>.
20. K. Stepanovic, J. Wu, R. Everhardt, and M. de Weerd, "Unlocking the Flexibility of District Heating Pipeline Energy Storage with Reinforcement Learning," *Energies* 2022, Vol. 15, Page 3290, vol. 15, no. 9, p. 3290, Apr. 2022, <https://doi.org/10.3390/EN15093290>.
21. L. Merkert, A. Abdoul Haime, and S. Hohmann, "Optimal Scheduling of Combined Heat and Power Generation Units Using the Thermal Inertia of the Connected District Heating Grid as Energy Storage," *Energies* 2019, Vol. 12, Page 266, vol. 12, no. 2, p. 266, Jan. 2019, <https://doi.org/10.3390/EN12020266>.
22. S. Wang, Q. Guan, Q. Wu, and M. Zhang, "A new business model for coordinated operation of wind power plant and flexible district heating system," *IET Conference Proceedings*, vol. 2022, no. 11, pp. 70–74, Jan. 2022, <https://doi.org/10.1049/ICP.2022.1668>.
23. J. Yang, N. Zhang, A. Botterud, and C. Kang, "On An Equivalent Representation of the Dynamics in District Heating Networks for Combined Electricity-Heat Operation," *IEEE Transactions on Power Systems*, vol. 35, no. 1, pp. 560–570, Jan. 2020, <https://doi.org/10.1109/TPWRS.2019.2935748>.
24. O. Arslan and A. E. Arslan, "Performance evaluation and multi-criteria decision analysis of thermal energy storage integrated geothermal district heating system," *Chemical engineering research & design*, vol. 167, pp. 21–33, Sep. 2022, <https://doi.org/10.1016/J.PSEP.2022.08.073>.
25. J. Röder, B. Meyer, U. Krien, J. Zimmermann, T. Stühmann, and E. Zondervan, "Optimal Design of District Heating Networks with Distributed Thermal Energy Storages – Method and Case Study," *International Journal of Sustainable Energy Planning and Management*, vol. 31, pp. 5–22, May 2021, <https://doi.org/10.5278/IJSEPM.6248>.
26. V. MEŞİN and A. KARAKAYA, "Contribution of Geothermal Resources that Could Be Used in District Heating System to Türkiye Economy and Analysis in terms of Carbon Emissions,"

- Politeknik Dergisi*, vol. 26, no. 1, pp. 345–355, Jan. 2023, <https://doi.org/10.2339/POLITEKNIK.1104204>.
27. D. Romanov and B. Leiss, “Geothermal energy at different depths for district heating and cooling of existing and future building stock,” *Renewable & Sustainable Energy Reviews*, vol. 167, pp. 112727–112727, Oct. 2022, <https://doi.org/10.1016/J.RSER.2022.112727>.
 28. “Scenarios for Integration of Medium-depth Geothermal in an Evolving District Heating System Case Study Geneva, Switzerland,” Accessed: Apr. 13, 2024. [Online].
 29. E. Hałaj, J. Kotyza, M. Hajto, G. Pełka, W. Luboń, and P. Jastrzębski, “Upgrading a District Heating System by Means of the Integration of Modular Heat Pumps, Geothermal Waters, and PVs for Resilient and Sustainable Urban Energy,” *Energies (Basel)*, vol. 14, no. 9, p. 2347, Jan. 2021, <https://doi.org/10.3390/EN14092347>.
 30. D. xi Liu, H. Y. Lei, J. S. Li, C. shan Dai, R. Xue, and X. Liu, “Optimization of a district heating system coupled with a deep open-loop geothermal well and heat pumps,” *Renew Energy*, vol. 223, p. 119991, Mar. 2024, <https://doi.org/10.1016/J.RENENE.2024.119991>.
 31. S. Nielsen *et al.*, “Smart Energy Aalborg: Matching End-Use Heat Saving Measures and Heat Supply Costs to Achieve Least Cost Heat Supply,” *International Journal of Sustainable Energy Planning and Management*, vol. 25, pp. 13–32, Jan. 2020, <https://doi.org/10.5278/IJSEPM.3398>.
 32. B. Möller and S. Nielsen, “High resolution heat atlases for demand and supply mapping,” *International Journal of Sustainable Energy Planning and Management*, vol. 1, pp. 41–58, 2014, <https://doi.org/10.5278/IJSEPM.2014.1.4>.
 33. N. Putkonen *et al.*, “Modeling the Baltic countries’ Green Transition and Desynchronization from the Russian Electricity Grid,” *International Journal of Sustainable Energy Planning and Management*, vol. 34, pp. 45–62, May 2022, <https://doi.org/10.54337/IJSEPM.7059>.
 34. A. Feldman-Olszewska A., T. Adamczak-Biały, A. Becker, Characterization of the Jurassic and Triassic reservoirs and seals from North Mazovia as a candidate site for CO₂ storage based on data from deep boreholes (in polish). Bulletin of Polish Geological Institute (PIG) 448:27-46, 2012.